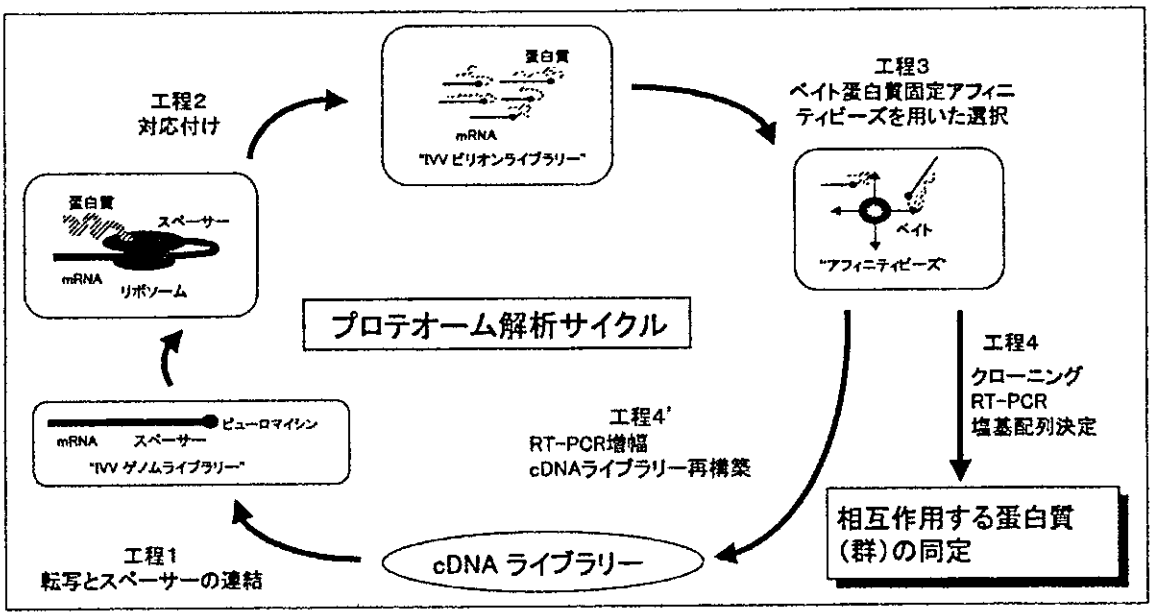

図 4 IVV を用いたプロテオーム解析

込まれることを見いだした[14].

ピューロマイシンやその誘導体が，リボソームで翻訳途中の蛋白質のC末端にランダムに取り込まれることは知られていたが，全長蛋白質のC末端に特異的結合することは，新しい知見であった．この現象は，図3に示すようなモデルで説明できると考えている[11,14]．すなわち，ピューロマイシンが高濃度では，アミノアシル-tRNA と競合し，翻訳の途中でもリボソームのAサイトに入ることができ，翻訳途中の短鎖長蛋白質と結合する(図3a)．

一方，ピューロマイシンが低濃度の場合，翻訳途中ではアミノアシル-tRNA が優先的にAサイトに入り，ピューロマイシンは翻訳途中の蛋白質とは結合できない．ところが，終止コドンにリボソームが到着したときには，アミノアシル-tRNA がAサイトには存在しないので，ピューロマイシンはAサイトに入ることが可能になり，その結果，C末端にピューロマイシンが結合した全長蛋白質が生成される(図3b)．

以上の知見は，全長蛋白質のC末端に mRNA を結合させるという，IVV の構築に大きな意義があった．ピューロマイシンが任意の個所で翻訳途中の蛋白質と結合してしまうと，全長蛋白質と結合していない，機能を持たない可能性が大きい対応付け分子が主生成物として得られるようになってしまう．しかし，mRNA の3'末端に適当なスペーサーを介しピューロマイシンを連結した人工遺伝子を作製し，*in vitro* 蛋白質発現系に加えると，全長蛋白質のC末端に mRNA の3'末端が結合した対応付け分子が得られた．このようにして生み出されたのが IVV である[6]．

研究当初の構成であるスペーサー部分に，オリゴDNA を使用した場合は，IVV の生成効率(対応付け効率)は数%であった．その後，スペーサー部分に改良を加え，DNA より柔軟な構造を持つポリエチレングリコール(PEG)を使用した場合，対応付け効率が上昇し，現在では最大70%程度の対応付け効率で IVV を得ている[15]．この対応付け効率はライブラリーサイズに密接に関連し，最大 1×10^{14}/ml 程度の大きな対応付け分子のライブラリーを作製できる．IVV は，*in vitro* の蛋白質発現系を利用しているため，細胞毒性を持つ蛋白質も発現でき，また，蛋白質-mRNA 間の結合が安定な共有結合であるため，蛋白質の機能スクリーニングを非常に厳しい条件下でも行うことができる．また，同様の mRNA-蛋白質の対応付け手法として mRNA-protein fusion (mRNA ディスプレイ)法も，筆者らの報告の数カ月後に報告されている[16]．

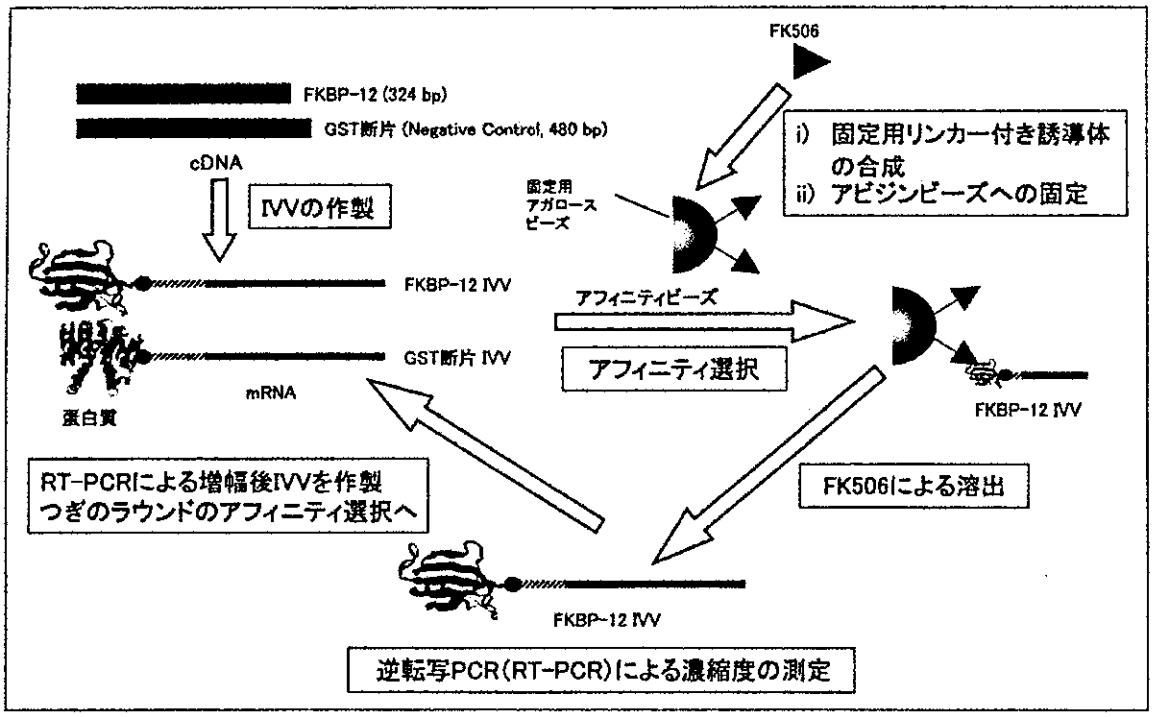

図 5　FKBP-12・FK 506 を用いたモデル系でのアフィニティ選択

IVV を用いたプロテオーム解析

ポストゲノムシーケンス時代のゲノム研究において，遺伝子の機能解析は重要なテーマである．筆者らは，遺伝子機能解析を目的とした，IVV を用いた網羅的な蛋白質間の相互作用(プロテオーム)解析法の開発を行っている．プロテオーム解析における IVV の応用の原理を図 4 に示す．以下の 1～4 の各工程を実行することにより，プロテオーム解析が実現される[10~12]．

1．細胞や組織由来の cDNA ライブラリーやカタログ化された cDNA より転写した mRNA の 3' 末端に，スペーサーに結合したピューロマイシンを連結させ，IVV 遺伝子型(IVV ゲノム)のライブラリーを作製する．
2．IVV ゲノムを無細胞翻訳系(*in vitro* の蛋白質発現系)に加え，蛋白質の合成を行い，表現型である蛋白質と IVV ゲノムが連結された IVV 対応付け分子(IVV ビリオン)のライブラリーを作製する．
3．相互作用を調べたい蛋白質(餌という意味でベイトと通常よばれる)を固定したアフィニティビーズを調製する．上記の IVV ビリオンのライブラリーを，アフィニティ選択の要領で，吸着させたのち，相互作用した IVV ビリオンを回収する．
4．回収した IVV ビリオンを逆転写 PCR(RT-PCR)により増幅し，クローニング後，DNA 配列解析を行い，ベイトに相互作用した蛋白質の配列解析を行う．
4'．3 で回収された蛋白質(IVV ビリオン)の濃縮度が十分でなく，同定が困難の場合，RT-PCR により増幅した DNA より，再度 IVV ビリオンライブラリーを作製し，工程 3 のアフィニティ選択を実行する．

以上のような，IVV を用いたプロテオーム解析法の特徴としては，IVV は蛋白質の情報タグとして mRNA を持つため，配列解析が容易な核酸(mRNA を逆転写した cDNA の配列を解析)を蛋白質の同定に利用できる点，プロテオーム解析のサイクルを複数回繰り返す(複数ラウンドの選択を行う)ことにより，相互作用する蛋白質の濃縮度を上げることがで

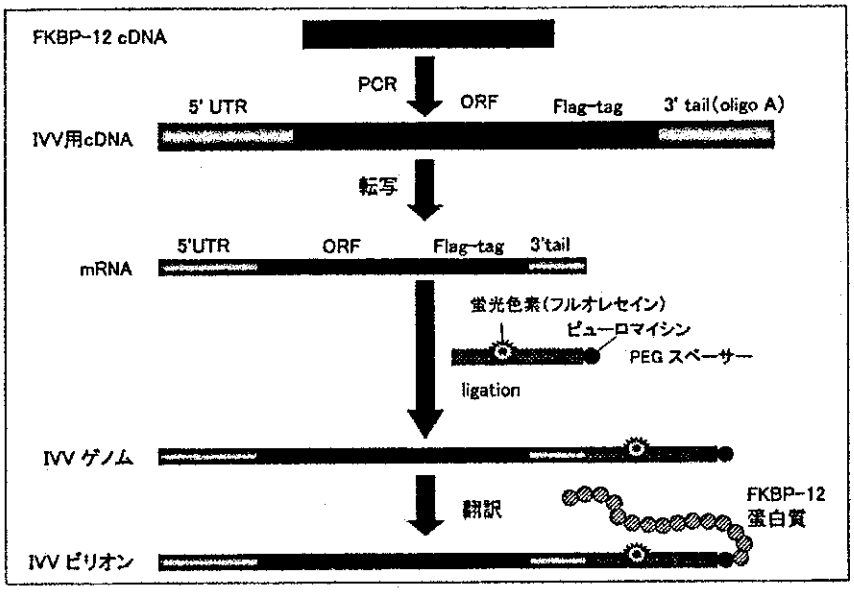

図 6
FKBP-12 IVV の作製

きる点があげられる．このような特徴により，二次元電気泳動-質量分析法などを用いた，従来のプロテオーム解析法の欠点を改善した手法を，IVV を用いることにより確立できる．

薬剤-蛋白質相互作用の網羅的解析

ヒトゲノム配列の解明により，いわゆるゲノム創薬がさまざまな場所で大きく取り上げられ，期待が増している．ゲノム科学の進歩で，病態における遺伝子発現の変動が，DNA チップやプロテオーム解析などにより，調べられるようになってきた．このような手法により，疾患の新たなマーカー蛋白質が発見されたり，SNP 解析により治療効果や副作用を各個人レベルで予測できたりするようになる[17]．

しかしながら，医薬品開発の研究に直接的に必要なのは，疾患マーカーや SNP 解析結果ではなく，薬剤ターゲット蛋白質とその阻害(あるいは作動)薬である．これまでも，ゲノム配列よりオーファン GPCR や未知のキナーゼなどが，新たな薬剤ターゲットになるのではないかという予想のもとに研究されているが，一つひとつを調べる方法は非効率である．

前項では，IVV を用いた蛋白質-蛋白質相互作用を網羅的に解析(プロテオーム解析)する手法について述べたが，筆者らは，薬剤-蛋白質相互作用も IVV 法を用いて網羅的に解析できると考えている．すなわち，既存薬剤やファーマコフォアをベイトに用いたアフィニティ選択により，薬剤と相互作用する蛋白質(群)の網羅的な解析が期待でき，新たな薬剤ターゲット蛋白質の発見につながると考えられる．

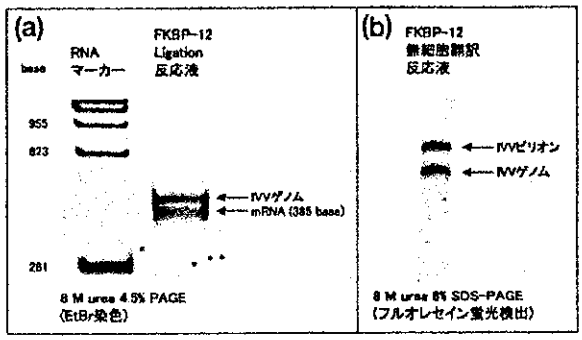

図 7 FKBP-12 mRNA と IVV のポリアクリルアミドゲル電気泳動

筆者らは，IVV 法を用いた薬剤-蛋白質相互作用解析のモデル系として，FK 506-FK 506 結合蛋白質(FKBP-12)[18]のアフィニティ選択実験を行った(図 5)．

1．FKBP-12 IVV ビリオンの作製(図 6)

クローニングされた FKBP-12 の cDNA をもとに，PCR により，IVV 形成に必要な 5' 側非翻訳領域

(5'UTR：プロモーター配列など)と3'tail(oligoAなど)を付加後，転写し，mRNAを作製した．つぎに，ピューロマイシンを末端に持つポリエチレングリコール含有スペーサー(PEGスペーサー)をRNAリガーゼで連結し，IVVゲノムを得た．ここで，PEGスペーサーには，IVVピリオンの生成効率(対応付け効率)を測定するために行う，ゲル電気泳動の蛍光検出の目的で，蛍光色素(フルオレセイン)を導入してある．得られたIVVゲノムをコムギ胚芽由来無細胞翻訳系に加え，FKBP-12蛋白質のC末端がmRNAの3'末端に連結されたIVVピリオンを得た．

ライゲーションと無細胞翻訳の反応液のゲル電気泳動結果を図7に示す．PEGスペーサーとmRNAの連結効率(IVVゲノムの収率)は60%程度(図7a)，対応付け効率は50%程度(図7b)であった．

2．FK 506固定アガロースビーズを用いたFKBP-12 IVVのアフィニティ選択

FKBP-12と結合する薬剤であるFK 506を固定したアガロースビーズを用い，FKBP-12 IVVピリオンのアフィニティ選択実験を行った(図5)．FKBP-12とネガティブコントロールにglutation-S-transferase(GST)の断片蛋白質(160アミノ酸)のIVVピリオンを用い，それぞれ1 pmolを1：1の割合で混合し，FK 506固定アガロースビーズに加え，IVVピリオンをアフィニティ吸着させた．ついでビーズを洗浄後，0.2 mM FK 506溶液でIVVを溶出した．投入したIVV溶液(input)と溶出液(溶出1回目，2回目，3回目)をRT-PCRし，含有しているFKBP-12とGSTの割合を，アガロース電気泳動で調べた(図8)．

RT-PCRは，FKBP-12(385 base)とGST(541 base)IVV RNAの共通配列部分である5'UTRと3'tail部分をプライマーに用い，双方が同時に同程度増幅されるようにした．各溶液のRT-PCR(30 cycles)後のアガロース電気泳動の結果，inputではFKBP-12とGSTの双方のバンドがほぼ1：1の濃度で検出されたのに対し，溶出液にはFKBP-12のバンドだけが検出され，FKBP-12のIVVが選択的に吸着・溶出されたことがわかる．

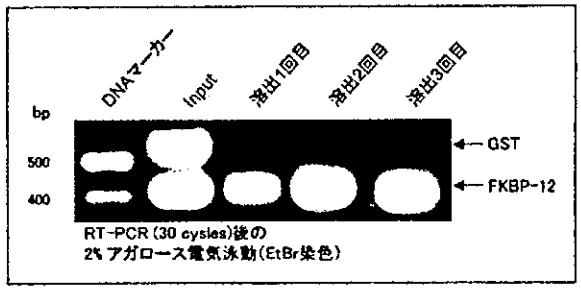

図8 アフィニティ選択各溶液のRT-PCR
(FKBP-12対GSTの比を1：1でinputした場合)

表1 リアルタイムRT-PCRによる濃縮率の定量
(FKBP-12対GSTの比を1：1でinputした場合)

Sample	Copies/μL FKBP	Copies/μL GST	比 (FKBP/GST)	濃縮率*
Input	1.1×10^{8}	1.6×10^{8}	1/1.5	—
溶出1	7.4×10^{3}	3.1×10^{2}	24	34
溶出2	5.4×10^{3}	2.3×10^{2}	23	33
溶出3	5.9×10^{4}	4.5×10^{2}	130	190

*濃縮率は各sampleの比をinputのそれで除した数値
Inputに対するFKBP-12の濃縮率を示す．

つぎに，各溶液に含有しているFKBP-12とGSTのRNAを定量するため，リアルタイムPCR装置による測定を行った．リアルタイムRT-PCRによる定量は，FKBP-12あるいはGSTに選択的なプライマーを用いた，100 bp程度の鎖長を増幅できる系を構築し行った．それぞれ，テンプレートRNAが10～10^{9}copies/μLで定量性が得られる系を構築することができた．リアルタイムRT-PCRで定量した結果，inputでは，FKBP-12のRNAが1.1×10^{8}copies/μL，GSTのRNAが1.6×10^{8}copies/μLでそれぞれ存在(FKBP-12：GST＝1：1.5)するのに対し，溶出3回目の溶液には，FKBP-12(5.9×10^{4}copies/μL)とGST(4.5×10^{2}copies/μL)がそれぞれ存在し，FKBP-12がGSTに対し190倍選択的に濃縮されていた(表1)．

3．IVVライブラリーモデルでのFKBP-12 IVVのアフィニティ選択

実際のスクリーニングに用いる，細胞や組織より抽出したmRNAより作製したIVVライブラリーは，多様な蛋白質-核酸対応付け分子の混合物であり，極微量の薬剤と相互作用するIVVを含有して

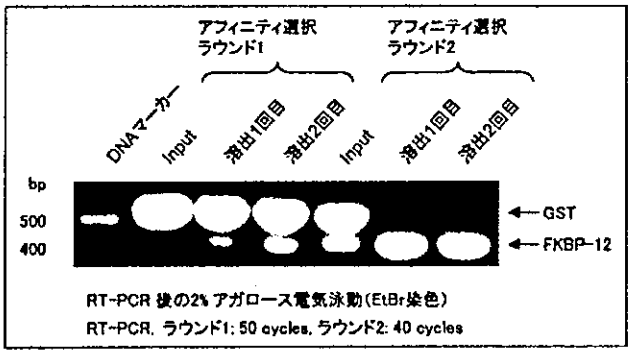

RT-PCR 後の2% アガロース電気泳動(EtBr染色)
RT-PCR, ラウンド1: 50 cycles, ラウンド2: 40 cycles

図 9 アフィニティ選択各溶液の RT-PCR
(FKBP-12 対 GST の比を 1：10,000 で input した場合)

表 2 リアルタイム RT-PCR による濃縮率の定量
(FKBP-12 対 GST の比を 1：10,000 で input した場合)

Sample	Copies/μL FKBP	Copies/μL GST	比 (FKBP/GST)	濃縮率*
ラウンド 1				
Input	1.7×10^{4}	2.8×10^{8}	1/16000	—
溶出 1	1.5×10^{2}	5.3×10^{3}	1/35	450
溶出 2	7.0×10^{1}	5.1×10^{2}	1/7	2300
ラウンド 2				
Input	2.3×10^{7}	4.7×10^{8}	1/20	—
溶出 1	3.2×10^{4}	4.3×10^{2}	75	1.2×10^{6}
溶出 2	1.4×10^{5}	1.1×10^{3}	125	2.0×10^{6}

*濃縮率は各 sample の比をラウンド 1 の input の比で除した数値
ラウンド 1 の input に対する FKBP-12 の濃縮率を示す.

いるにすぎない. 前述したように, IVV を用いたプロテオーム解析法の特徴として, 選択ラウンドを複数回行うことにより, 相互作用する IVV が相乗的に濃縮されることが期待される.

ここでは, 多量の夾雑 IVV 存在下, 微量の特異的結合 IVV が濃縮されるか, また, 複数回の選択ラウンドによる相乗的な濃縮が認められるか, それらを検証する目的で, FKBP-12 と GST の IVV を 1：10,000 の割合で混合し, アフィニティ選択を 2 ラウンド行った. 各ラウンドのアフィニティ選択時の各溶液の RT-PCR(ラウンド 1：50 cycles, ラウンド 2：40 cycles)後のアガロース電気泳動の結果を図 9 に, リアルタイム RT-PCR で FKBP-12 と GST の RNA を定量した結果を表 2 に示す. ラウンド 1 の input では, RT-PCR 後のアガロース電気泳動で GST のバンドだけが認められるが, 溶出液では FKBP-12 のバンドも検出されるようになり, FKBP-12 の選択的濃縮が認められた. リアルタイム RT-PCR の定量では, FKBP-12 の GST に対する濃縮率は 2,300 倍であった.

ラウンド 1 での溶出液を RT-PCR(35 cycles)で増幅し, 引きつづき転写, PEG スペーサーとの RNA リガーゼによる連結, コムギ無細胞翻訳系での対応付けを行い, ラウンド 2 のアフィニティ選択に用いる IVV を作製した. ラウンド 2 の input IVV の FKBP-12 に対する GST の比率は 1：20 であった. 2 ラウンド目のアフィニティ選択を行ったあとの, RT-PCR(40 cycles)後のアガロース電気泳動では, FKBP-12 のバンドがほぼ単一で検出されるようになり, 相乗的な FKBP-12 の選択的濃縮が確認できた. リアルタイム RT-PCR による定量では, 2 ラウンド全体で 2×10^{6}倍, FKBP-12 が GST に対し濃縮されていた.

以上のように, IVV を利用した薬剤-蛋白質相互作用解析の有用性が, FK 506•FKBP-12 を用いたモデル系で確認できた. 現在, 組織由来の cDNA ライブラリーより IVV ピリオンライブラリーを作製し, FK 506 やゲフィチニブなどいくつかの薬剤について, 相互作用する蛋白質の網羅的な解析を進めている.

おわりに

筆者らは, 蛋白質と mRNA が対応付けられた分子である IVV を提唱し, ピューロマイシンを利用した IVV の効率的な作製法を確立した. 現在では 1×10^{14}/ml 程度の大きな多様性を持つ, 対応付け分子ライブラリーを作製できるようになっており, IVV はプロテオーム解析の有用なツールになることが期待される.

IVV を用いたプロテオーム解析法は, IVV が情報タグとしての核酸部分を持つため, 相互作用した蛋白質の配列解析が非常に容易である点, 選択ラウンドを複数回行うことにより, 相互作用する蛋白質を濃縮することができる点でユニークである. IVV を用いた手法は, 蛋白質-蛋白質間の相互作用解析だけでなく, 薬剤-蛋白質間の相互作用解析にも有用であり, 新たな薬剤ターゲット蛋白質の発見や, 薬剤

の作用機序ならびに副作用機序の解明に応用可能である．

現在，筆者らは，ヒトやマウスのいくつかの組織由来のcDNAライブラリーよりIVVライブラリーを作製し，さまざまなベイト蛋白質や薬剤を用いたスクリーニングを実施中である．今後，このようなIVVライブラリーを用いたスクリーニングにより，遺伝子の機能解析や新たな薬剤ターゲット蛋白質の発見が迅速に行うことが可能になると考えている．

本研究の一部は，厚生労働省の厚生労働科学研究費補助金萌芽的先端医療技術推進研究事業(トキシコゲノミクス分野)の一環として行われた．

文　献

1) http://www.genome.gov/11006929
2) Kennedy GC, Matsuzaki H, Dong S, Lui W, Huang J et al.：Large-scale genotyping of complex DNA. Nat Biotechnol Published online：7, September 2003, doi：10. 1038/nbt 869.
3) Clarke PA, te Poele R, Wooster R, Workmana P：Gene expression microarray analysis in cancer biology, pharmacology, and drug development：progress and potential. Biochem Pharmacol 62：1311-1336, 2001.
4) Orphanides G：Toxicogenomics：challenges and opportunities. Toxicol Lett 140-141：145-148, 2003.
5) Shimizu N, Sugimoto K, Tang J, Takeyuki Nishi T, Sato I et al.：High-performance affinity beads for identifying drug receptors. Nat Biotechnol 18：877-881, 2000.
6) Nemoto N, Etsuko Miyamoto-Sato E, Husimi H, Yanagawa H：*In vitro* virus：Bonding of mRNA bearing puromycin at the 3'-terminal end to the C-terminal end of its encoded protein on the ribosome *in vitro*. FEBS Lett 414：405-408, 1997.
7) Ito T, Chiba T, Ozawa R, Yoshida M, Hattori M et al.：A comprehensive two-hybrid analysis to explore the yeast protein interactome. Proc Natl Acad Sci USA 98：4569-4574, 2002.
8) Scott JK, Smith GP：Searching for peptide ligands with an epitope library. Science 249：386-390, 1990.
9) Hanes J, Pückthun A：*In vitro* selection and evolution of functional proteins by using ribosome display. Proc Natl Acad Sci USA 94：4937-4942, 1997.
10) 宮本悦子，柳川弘志：*In vitro* virus法によるタンパク質間相互作用と遺伝子ネットワーク解析．プロテオミクス．(伊藤隆司，谷口寿章・編)，中山書店，2000，p 136-145.
11) 宮本悦子，柳川弘志：ピューロマイシンの進化分子工学と遺伝子ネットワーク解析への応用．蛋白質 核酸 酵素 46(2)：138-147，2001.
12) 宮本悦子，柳川弘志：*In vitro* virusおよび蛋白質C末端ラベル化法のポストゲノム研究への応用．蛋白質 核酸 酵素 48(11)：1474-1480，2003.
13) Yamolinsky MB, De La Haba GL：Inhibition by puromycin of amino acid incorporation into protein. Proc Natl Acad Sci USA 45：1721-1729, 1959.
14) Miyamoto-Sato E, Nemoto N, Kobayashi K, Yanagawa H：Specific bonding of puromycin to full-length protein at the C-terminus. Nucleic Acids Res 28：1176-1182, 2000.
15) Miyamoto-Sato E, Takashima H, Fuse S, Sue K, Ishizaka M et al.：Highly stable and efficient mRNA templates for mRNA-protein fusions and C-terminally labeled proteins. Nucleic Acids Res 31：e 78, 2003.
16) Roberts RW, Szostak JW：RNA-peptide fusions for the *in vitro* selection of peptides and proteins. Proc Natl Acad Sci USA 94：12297-12302, 1997.
17) 辻本豪三：遺伝子多形と薬剤の応答性．ゲノム創薬．(古谷利夫，増保安彦，辻本豪三・編)，中山書店，2001，p 164-177.
18) Maki N, Sekiguchi F, Nishimaki J, Miwa K, Hayano T et al.：Complementary DNA encoding the human T-cell FK 506-binding protein, a peptidylprolyl *cis-trans* isomerase distinct from cyclophilin. Proc Natl Acad Sci USA 87：5440-5443, 1990.

Published online December 2, 2004

Nucleic Acids Research, 2004, Vol. 32, No. 21 ***e169***
doi:10.1093/nar/gnh167

In vitro selection of Jun-associated proteins using mRNA display

Kenichi Horisawa, Seiji Tateyama, Masamichi Ishizaka, Nobutaka Matsumura, Hideaki Takashima, Etsuko Miyamoto-Sato, Nobuhide Doi and Hiroshi Yanagawa*

Department of Biosciences and Informatics, Faculty of Science and Technology, Keio University, Yokohama 223-8522, Japan

Received October 5, 2004; Revised and Accepted November 11, 2004

ABSTRACT

Although yeast two-hybrid assay and biochemical methods combined with mass spectrometry have been successfully employed for the analyses of protein–protein interactions in the field of proteomics, these methods encounter various difficulties arising from the usage of living cells, including inability to analyze toxic proteins and restriction of testable interaction conditions. Totally *in vitro* display technologies such as ribosome display and mRNA display are expected to circumvent these difficulties. In this study, we applied an mRNA display technique to screening for interactions of a basic leucine zipper domain of Jun protein in a mouse brain cDNA library. By performing iterative affinity selection and sequence analyses, we selected 16 novel Jun-associated protein candidates in addition to four known interactors. By means of real-time PCR and pull-down assay, 10 of the 16 newly discovered candidates were confirmed to be direct interactors with Jun *in vitro*. Furthermore, interaction of 6 of the 10 proteins with Jun was observed in cultured cells by means of co-immunoprecipitation and observation of subcellular localization. These results demonstrate that this *in vitro* display technology is effective for the discovery of novel protein–protein interactions and can contribute to the comprehensive mapping of protein–protein interactions.

INTRODUCTION

Comprehensive analysis of protein–protein interactions is an important task in the field of proteomics, functional genomics and systems biology. Protein–protein interactions are usually analyzed by means of biochemical methods such as pull-down assay and co-immunoprecipitation, yeast two-hybrid (Y2H) assay and phage display. Recently, the combined use of mass spectrometry (MS) with an affinity tag (1) has made the biochemical methods more comprehensive and reliable. However, the testable interaction conditions are restricted by the properties of the biological sources. The Y2H assay is one of the major tools used in the discovery and characterization of protein–protein interactions (2). However, the results of Y2H analyses often include many false positives due to auto-activating bait or prey fusion proteins (3) and interactions of proteins that are toxic to yeast cells cannot be examined. Phage display, the most widely used display technology (4), is an effective alternative, because the interactions between libraries and target proteins occur *in vitro*, allowing optimal conditions to be used for many different target proteins. Further, very low copy number proteins can be identified by repeating the selection round. However, the use of phage display is similarly limited, because phage libraries are produced in living bacteria (5).

Totally *in vitro* display technologies such as ribosome display (6,7), mRNA display (8–10) and DNA display (11) can circumvent the above difficulties, because they do not need living cells. In mRNA display, a library of genotype–phenotype linking molecules is constructed in which mRNA (genotype) binds to protein (phenotype) through puromycin during cell-free translation. After affinity selection via the protein moiety of the molecules in the library, the mRNA moiety of the selected molecules can be amplified by means of RT–PCR. By performing iterative selection, very low copy number proteins can be detected from large-scale cDNA libraries, routinely in the range of 10^{13} members. In 1997, the prototype of mRNA display was originally developed in our laboratory and that of Szostak independently, and the conjugate of protein with its encoding mRNA was named *in vitro* virus (IVV) (8,9) and RNA–peptide fusion (10), respectively. So far, RNA–peptide fusion has been applied to the selection of various functional peptides and antibody mimics (12,13), but the application to protein–protein interaction analysis has been limited (14,15). Recently, we improved the stability of the template mRNA for IVV molecules and the efficiency of IVV formation by employing a polyethylene glycol (PEG) spacer and wheat germ cell-free translation system (16) to improve the selection ability of the IVV technique. In this study, we applied the improved IVV technique to the screening of protein–protein interactions. As a model bait protein, we chose a basic leucine zipper (bZIP) domain of Jun protein, an important transcription factor, to screen Jun interactors from a mouse brain cDNA library. The screening afforded several known and unknown Jun-associated protein candidates, and we confirmed that many

*To whom correspondence should be addressed. Tel: +81 45 566 1775; Fax: +81 45 566 1440; Email: hyana@bio.keio.ac.jp

of the candidates interacted directly with Jun, not only *in vitro*, but also in cultured cells, by using pull-down assay and co-immunoprecipitation assay. These results demonstrate that our *in vitro* display technology is effective for discovery of novel protein–protein interactions and can contribute to the comprehensive mapping of protein–protein interactions.

METHODS

Preparation of bait template RNA

The cDNA of mouse Jun (167–319 amino acids) was amplified by PCR using a forward primer (5′-CCGCGGGATCCCCG-GTCTACGCCAACCTC-3′) containing a BamHI site and a reverse primer (5′-CACCCCTCGAGAACGTGGTTCATGA-CTTTCTGCTTA-3′) containing an XhoI site, and digested with BamHI and XhoI. The fragment was subcloned into the BamHI/XhoI site of pCMV-CBPzz vector (16), which contains a SP6 promoter, a part of the omega sequence named O′ (5′-ACAATTACTATTTACAATTACA-3′) (17), an N-terminal T7-tag coding sequence, and a C-terminal TAP tag coding sequence (1). From the resulting plasmid pCMV-JunCBPzz, a bait template DNA was PCR-amplified with primers 5′SP6(0′)T7 (5′- GAATTTAGGTGACACTAT-AGAAACAATTACTATTTACAATTACAATGGCTAGCA-TGACTGGTGGACAG-3′) and 3′FosCBPzz (5′-GGATCTC-CATTCGCCATTCA-3′). The PCR product was purified with a QIAquick PCR purification kit (Qiagen). The purified DNA was used as a template for *in vitro* transcription with a RiboMax large-scale RNA production system-SP6 (Promega). The RNA was purified with an RNeasy mini kit (Qiagen).

Preparation of IVV template RNA library

The architecture of IVV was described previously (16). Mouse brain poly(A)$^+$ RNA (BD Biosciences) was primed using the oligonucleotide 5′-TCGTCATCGTCCTTGTA-GTCAAGCTTN$_9$-3′ and cDNA was synthesized using a SuperScript double strand cDNA synthesis kit (Invitrogen). The cDNA was ligated with adaptor DNA (forward oligo-nucleotide: 5′-TAGCATGACTGGTGGACAGCAAATGGGT-GCGGCCGCGAATTCC-3′; reverse oligonucleotide: 5′-GGA-ATTCG-3′) using a Ligation High kit (Toyobo). After ethanol precipitation, the ligated DNA was PCR-amplified with primers, 5′F3 (5′-GGAAGATCTATTTAGGTGACACTATAGAACAA-CAACAACAACAAACAACAACAAAATG-3′) and 3′lib_PCR (5′-TTTTTTTTCTTGTCGTCATCGTCCTTGTAGTC-3′). The PCR product was purified with the QIAquick PCR purification kit and fractionated (over ~200 bp) with a CHROMA SPIN-1000 (BD Biosciences). The fractionated PCR product was used as a template for transcription using the RiboMax large RNA production system-SP6. The resulting RNA was ligated with PEG Puro spacer [p(dCp)2-T(Fluor)p-PEGp-(dCp)2-puromycin] using T4 RNA ligase (Takara). The ligated RNA was purified with the RNeasy mini kit.

Affinity screening

The IVV formation reaction was performed as described previously (16), with some modifications. Briefly, a 50 µl aliquot of wheat germ extract reaction mixture (Promega) containing 10 pmol of the bait Jun RNA, 10 pmol of the ligated library RNA, 80 µM amino acid mixture, 76 mM potassium acetate and 40 U of RNase inhibitor (Invitrogen) was incubated for 1 h at 26°C. Subsequently, the reaction mixture was added to 50 µl of rabbit immunoglobulin G (IgG) agarose beads (Sigma) equilibrated with 50 µl of IPP150 buffer (10 mM Tris–HCl, pH 8.0, 150 mM NaCl and 0.1% NP-40), and mixed on a rotator for 2 h at 4°C. The beads were washed with 800 µl of IPP150 buffer once and with 800 µl of TEV cleavage buffer (10 mM Tris–HCl, pH 8.0, 150 mM NaCl, 0.1% NP-40, 0.5 mM EDTA and 1 mM DTT) five times, then 100 µl of TEV cleavage buffer containing 100 U of TEV protease was added, and rotation was continued for 2 h at 16°C. The resulting eluate was used as the RT–PCR template. RT–PCR was performed with a OneStep RT–PCR kit (Qiagen) using primers, 5′F3 and 3′Flag-1AL (5′-TTTTTTTTCTTGTCGTCATCG-TCCTTGTAG-3′). The optimal number of PCR cycles without reaching a plateau was 26–30 cycles at each RT–PCR step. The RT–PCR product was used for the next round of selection as described above. After five rounds of affinity screening, the RT–PCR product was cloned using a PCR cloning kit (Qiagen) and sequenced with an ABI PRISM 3100 Genetic Analyzer (Applied Biosystems).

Sequence analysis

The selected clones were subjected to nucleotide–nucleotide BLAST (BLASTN) search (18) to identify the protein represented by each clone. The nucleotide database obtained from the NCBI ftp site (ftp://ftp.ncbi.nlm.nih.gov/blast/db/) was employed as a reference database. The threshold of the *E*-value was configured at 1.0×10^{-1}. Clustering of the clones was performed using the CLUSTALW program (19).

Real-time PCR analysis

Real-time PCR were performed with LightCycler FastStart DNA master SYBR green I kit (Roche) and protein-specific primer sets (Supplementary Table 1) on the LightCycler (Roche). The standard template DNA was PCR-amplified from each selected sequence on pDrive vectors (Qiagen) using primers, 5′M13F (5′-GTTTTCCCAGTCACGACGTTG-3′) and 3′M13R (5′-GAAACAGCTATGACCATGATTACG-3′).

Pull-down assay

Pull-down assay using the C-terminal fluorescence labeling technique was performed according to the method of Miyamoto-Sato *et al.* (16). The DNA templates were PCR-amplified from the cloned plasmids with primers, 5′F3 and 3′R3 (5′-TTTTTTTTCTCGAGCTTGTCGTCATCG-3′). The amplicons were used as templates for transcription. The resulting mRNAs were translated in the presence of fluorescence-labeled puromycin to make fluorescence-labeled proteins. Bait Jun was also translated in the cell-free translation system separately. These translated proteins were mixed together, incubated with rabbit IgG agarose beads, and washed as described above. The binding proteins were eluted with sample buffer (0.1 M Tris–HCl, pH 6.8, 4% SDS, 0.2% bromophenol blue and 20% glycerol) at 100°C for 5 min, subjected to 17.5% SDS–PAGE, and analyzed with a Molecular Imager FX (Bio-Rad Laboratories).

Co-immunoprecipitation assay

Full-length cDNA of Jun was inserted into a pCMV-Tag5 expression vector (Stratagene). DNA fragments of the selected proteins were subcloned into the pQBI25f expression vector (Qbiogene), in which the peptide linker has been replaced with a HL4 helix linker (20) and a C-terminal FLAG-tag added. Neuro2a cells were co-transfected with both pCMV-Tag5 coding Jun and pQBI25f coding each selected protein sequence or GFP-HL4-FLAG alone (mock) using LipofectAMINE2000 (Invitrogen). After 24 h, the cells in a 6 cm dish were rinsed once with ice-cold phosphate-buffered saline (PBS) and scraped using cell-scrapers with 1.5 ml of PBS. The cells in the suspension were collected by centrifugation at 5000 r.p.m. for 5 min and lysed in 375 µl of NP lysis buffer (20 mM Tris–HCl, pH 7.6, 150 mM NaCl, 1.0% NP-40, 50 mM NaF, 1 mM Na_3VO_4 and 2 mM EDTA) containing a Complete protease inhibitor cocktail (Roche) with sonication for 1 min at 170 W and rotation for 1 h at 4°C. The lysate was centrifuged at 15 000 r.p.m. for 15 min at 4°C. An aliquot of 15 µl of the supernatant was separated and used for western-blot analysis to compare protein expression levels. For co-immunoprecipitation, 30 µl of anti-FLAG M2 agarose beads (Sigma) was added to 350 µl of the cell lysate and the mixture was incubated 2 h at 4°C with rotation. Finally, the agarose beads were washed four times with lysis buffer and resuspended in SDS–PAGE loading buffer for immunoblot analysis.

For western-blot analysis, the polyacrylamide gel was transferred onto a PVDF membrane. Duplicate blots were made from the identical immunoprecipitation experiment. One blot was probed with a rabbit anti-Jun polyclonal antibody (Calbiochem) to detect co-immunoprecipitated Jun, and the other was probed with a rabbit anti-green fluorescent protein (GFP) polyclonal antibody (Molecular Probes) to monitor the amount of GFP- and FLAG-tagged selected proteins that had been immunoprecipitated by the anti-FLAG M2 agarose beads in each reaction. The blots were revealed by an ECF western blotting kit (Amersham Biosciences) and Molecular Imager FX.

Subcellular localization analysis

COS7 cells in a 3.5 cm glass dish were co-transfected with an expression vector pQBI25f coding each newly selected protein fragment interacting with Jun *in vitro*, selected Fos, or GFP-HL4-FLAG alone (mock), together with an expression vector pCMV-Tag5B coding full-length Jun, using LipofectAMINE2000 reagent for 24 h. Before observation, the transfected cells were treated with 100 ng/ml of Hoechst33342 (Molecular Probes) for 5 min to stain the nucleus. The cells transfected with each GFP-tagged protein were observed with an Axiovert 200 M system (Carl Zeiss).

Functional clustering using annotation data

The functional annotations of the selected proteins were searched in the entries under Gene Ontology (GO) in the Mouse Genome Informatics (MGI) website (http://www.informatics.jax.org/) and those under Refseq in the Locuslink website (http://www.ncbi.nlm.nih.gov/LocusLink/). The selected proteins were clustered based on the common terms of the annotations.

RESULTS

Preparation and confirmation of IVV template library

Figure 1A shows the principle of the formation of an IVV molecule, a conjugate of protein (phenotype) and RNA (genotype). A library of IVV molecules was constructed from a cDNA library derived from mouse brain poly(A)$^+$ RNA. Because each process in the IVV template construction, i.e. reverse transcription, ligation of the PEG Puro spacer, and especially PCR-amplification (21), can be a cause of bias, which may prevent enrichment of specifically selected clones, we confirmed that no significant bias had occurred in the process of construction of the IVV template library before affinity selection. We performed RT–PCR analysis for several genes with specific primers to compare the amounts in the original mouse brain poly(A)$^+$ RNA and the constructed IVV template RNA library: all genes tested were found in both libraries in almost equal amounts (data not shown). The result indicates that this IVV template library is suitable for selection. Indeed, this test of the library was critical for success in the selection of novel interactions.

Co-translation of IVV library and bait protein

As shown in Figure 1B, we employed cell-free co-translation of bait protein with the IVV library. This protocol does not require a separate preparation of bait proteins, as was performed in the previous study (14). Thus, we considered that this convenient approach would be more suitable for high-throughput screening for protein–protein interactions. We examined the optimal concentration of mRNA template for bait Jun (Figure 1C) to generate a sufficient amount of bait protein in a cell-free translation system. The largest amount of the bait protein (~10 ng/µl) was obtained when the mRNA concentration was 200 nM (data not shown).

Selection of Jun-associated proteins from cDNA library

We then applied the IVV selection system to discover Jun-associated proteins in the mouse brain cDNA library. We performed two different kinds of selection, one being selection of the IVV library in the presence of the Jun bait protein, and the other being selection in the absence of the bait protein. Co-translated bait protein with its interactors was captured by IgG agarose beads through the added affinity tag. After five rounds of selection, the resulting libraries were cloned and sequenced. Consequently, 217 clones were obtained from the 5th round library of the bait (+) selection, and 151 clones were obtained from the 5th round library of the bait (−) selection. In the bait (−) library, it seems that materials specifically bound to the rabbit IgG agarose beads are enriched, and thus we considered clones also detected in the bait (−) library to be false positives [50 of 217 clones in the bait (+) library were removed in this step]. This simple approach to remove false positives was lacking in the previous protocols of mRNA display (14) and other display technologies (22).

Also, 24 clones including stop codons were removed, because such clones cannot form IVV and thus cannot interact with the bait protein as an IVV containing a protein moiety. The remaining 143 clones were subjected to nucleotide-nucleotide BLAST (BLASTN) search to identify the coded

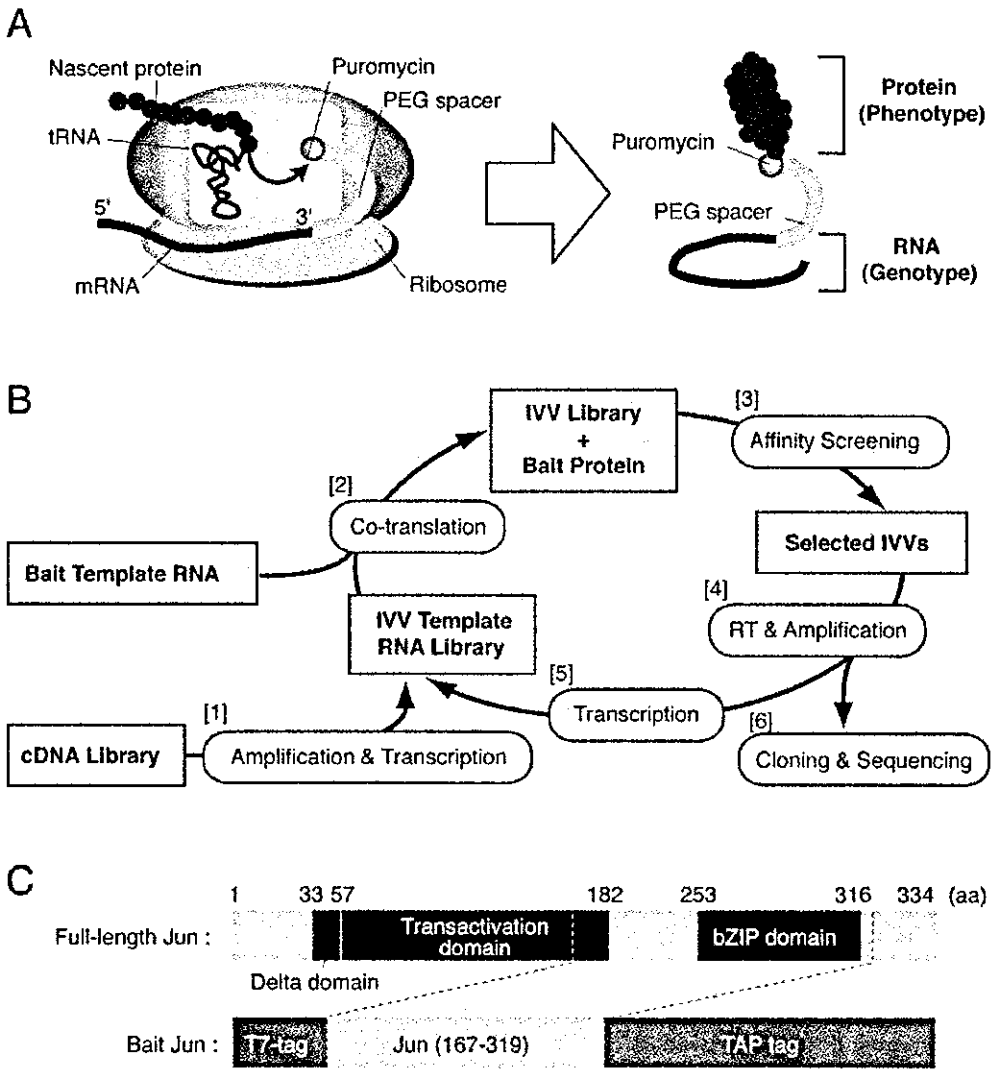

Figure 1. IVV selection of Jun-associated proteins. (A) Principle of IVV formation on the ribosome in a cell-free translation system (8). Puromycin ligated to the 3′-terminal end of mRNA through the polyethyleneglycol (PEG) spacer (16) can enter the ribosomal A site to bind covalently to the C-terminal end of the protein that it encodes. (B) Schematic representation of iterative selection for protein–protein interactions using IVV. [1] A cDNA library encoding various proteins is PCR-amplified, transcribed and ligated with a PEG spacer having puromycin. [2] The IVV template RNA library and bait template RNA are co-translated in a cell-free translation system. [3] The complex of bait protein and IVV library are subjected to affinity selection. [4] The RNA portion of the bound IVVs is reverse-transcribed and PCR-amplified. [5] The RT–PCR product is subjected to the next round of selection or [6] identified by cloning and sequencing. (C) Construction of the bait Jun for the selection. Jun protein has three conserved domains, delta domain, transactivation domain and bZIP domain. As a bait, the fragment containing the bZIP domain of Jun was fused with a T7-tag for confirmation of expression of the bait protein and with the TAP affinity selection tag, which contains the IgG binding domain of protein A, TEV protease cleavage site and calmodulin binding peptide (1).

proteins. Of the 143 clones, 7 were further removed, because these clones corresponded to 5′-untranslated region (5′-UTR) or 3′-UTR in mRNA sequences. Consequently, a total of 81 clones (37% of total clones) were eliminated from the obtained 217 clones as false positives. Surviving clones from the above examinations were further characterized.

The remaining 136 clones were clustered into 20 distinct sequence groups by the CLUSTALW algorithm (Table 1). Ten of the clusters consist of siblings, and the others consist of single clones (Table 1). BLASTN search revealed that 16 of the clusters involved known proteins. The other four proteins, 4732436F15Rik, 9130229H14Rik, 1200008A14Rik and B130050I23Rik, are hypothetical proteins, which have been reported in the full-length cDNA sequencing and functional annotation project 'FANTOM2' (23). Characterization of the amino acid sequences revealed that 14 of the 20 proteins contain leucine heptad repeats, which have the potential to form a leucine zipper motif. Four of the 20 proteins, Fos, Jun, Atf4 and Jdp2, have already been reported to interact with Jun directly (24), but the other 16 have not. Thus, we further examined their specific interactions with Jun by means of real-time PCR, *in vitro* pull-down assays and co-immunoprecipitation assays.

Table 1. A total of 20 selected proteins from IVV selection and sequence analyses

Gene symbol	Accession no.	Number of clones	Locus on mRNA sequence (base)	Previous report	Leucine heptad repeats	*In vitro* pull-down assay[a]
SNAP19	NM_183316.1	78	1...285	Unknown	Y	++
Kif5C (region C)	NM_008449.1	17	2473...2672	Unknown	Y	+
Kif5A (region C)	NM_008447.2	5	2654...2851	Unknown	Y	+
Eef1d	NM_023240.1	5	149...522	Unknown	Y	ND[b]
Jdp2	NM_030887.2	5	481...717	Known	Y	+++
Kif5C (region N)	NM_008449.1	4	907...1115	Unknown	N	—
Nef3	NM_008691.1	4	1086...1251	Unknown	N	—
4732436F15Rik	XM_143418.3	3	2087...2287	Unknown	Y	++
Fos	NM_010234.2	3	493...740	Known	Y	+++
9130229H14Rik	XM_135706.3	2	96...267	Unknown	Y	++
Atf4	NM_009716.1	1	1091...1305	Known	Y	+
Mapre3	NM_133350.1	1	724...980	Unknown	N	+
Cspg6	NM_007790.2	1	2474...2689	Unknown	Y	++
Mapk8ip3	NM_013931.1	1	1413...1624	Unknown	Y	+
Jun	NM_010591.1	1	904...1036	Known	Y	++
1200008A14Rik	NM_028915.1	1	1522...1677	Unknown	Y	+
GFAP	K01347.1	1	892...1025	Unknown	N	—
B130050I23Rik	NM_153536.2	1	1151...1424	Unknown	Y	++
Kif5A (region N)	NM_008447.2	1	1427...1463	Unknown	N	—
Kif5B (region N)	NM_008448.1	1	1229...1362	Unknown	N	—

[a]Interaction level of selected proteins with bait Jun based on the result of pull-down assay: —, none; +, weak; ++, strong; +++, very strong; and ND, no data.
[b]Eef1d contains leucine heptad repeats, and significant interaction was observed in the presence of bait protein, but similar behavior was also observed in the absence of bait protein.

Quantitative analysis of selected protein clones using real-time PCR

The finally selected clones may merely contain RNA that is abundant in the initial library, such as β-actin. Such negative clones can be distinguished from positive clones that are expected to be enriched in the bait (+) selection, but not enriched in the bait (−) selection. Thus, we used real-time PCR analysis to determine the amounts of the DNA molecules encoding the selected proteins in the DNA libraries from each round of the selection. Of the 20 candidates, 19 selected proteins were enriched in each round in the presence of Jun bait. The enrichment rates were between 80- and 2.0×10^4-fold, while β-actin (negative control) was not enriched. In contrast, none of the selected proteins, nor β-actin, was enriched in the bait (−) selection. These results support the conclusion that the 19 selected proteins were specifically enriched by interacting directly or indirectly with Jun bait protein. In the initial library and in the 5th bait (+), library the 19 proteins accounted for less than 0.1% and over 50% of the total, respectively. The region N of Kif5A with a chain length of 38 bp was not analyzed, because the clone was too short to perform real-time PCR analysis.

Verification of protein–protein interactions *in vitro* by pull-down assay

To determine whether the selected proteins have the ability to interact directly with Jun, *in vitro* pull-down assay was performed. A C-terminal-specific fluorescence labeling technique, which is a simple and convenient method (25), was employed for the pull-down assay. As shown in Table 1, 14 proteins including 4 known positives, Jun, Fos, Atf4 and Jdp2, exhibited direct interactions with Jun bait protein *in vitro*. All of the 14 proteins, except for Mapre3, contain leucine heptad repeats. The other proteins, Kif5A (region N), Kif5B (region N), Kif5C (region N), Nef3 and GFAP, except for Eef1d (see Table 1) neither interacted nor contained leucine heptad repeats. We considered that these proteins might interact with Jun indirectly via other Jun-associated proteins, because there are some findings indicating interactions between selected proteins. For example, regions C and N of Kif5 family (Kif5s) proteins (Table 1) are known to interact in a single molecule, generating a compact structure to control the motor activity of the Kif5s (26–28). The region C clones have leucine heptad repeats and interacted directly with Jun *in vitro*; thus, region N fragments of Kif5s might interact with bait Jun via region C fragments of Kif5s in this selection. Also, Nef3 are known to interact with Kif5A (29), and selected regions of Nef3 are highly homologous to parts of GFAP. Consequently, all five proteins for which direct interactions with Jun were not confirmed by pull-down assay, in spite of the specific enrichment confirmed by real-time PCR, may interact indirectly with Jun through other positive clones.

Verification of protein–protein interactions in cultured cells

Transfected Jun protein was assayed by co-immunoprecipitation with 10 GFP- and FLAG-tagged selected proteins which exhibited interaction with Jun *in vitro* (Figure 2). All 10 selected proteins were immunoprecipitated (Figure 2B, upper panels), while Jun was co-immunoprecipitated with only 6 of the 10 proteins, SNAP19, Cspg6, 9130229H14Rik, 1200008A14Rik, B130050I23Rik and 4732436F15Rik (Figure 2B, lower panels). The other four proteins, Kif5A (region C), Kif5C (region C), Mapk8ip3 and Mapre3, apparently did not interact with Jun.

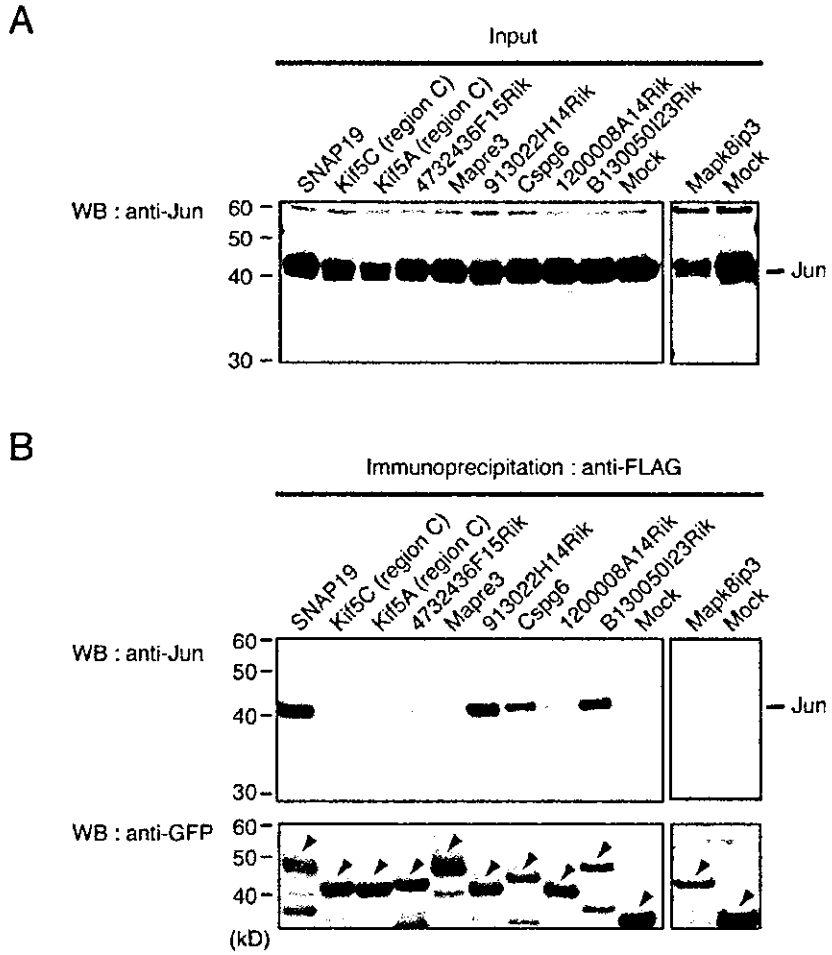

Figure 2. Co-immunoprecipitation assay between Jun and selected Jun-associated protein candidates. (A) Western-blot analysis, showing the expression levels of Jun after co-transfection with Jun and each of 10 selected proteins. 'Mock' was co-transfected with Jun and GFP-HL4-FLAG. (B) Extracts of COS7 cells which were transfected with Jun and each of the ten selected proteins were immunoprecipitated with anti-FLAG antibody. This was followed by western-blot analysis using the anti-Jun antibody to detect co-immunoprecipitated Jun protein (top) and anti-GFP antibody to detect GFP-fused selected proteins (arrowhead on the bottom).

Determination of subcellular localization of selected protein fragments

To elucidate why the interaction of some proteins that interacted with Jun *in vitro* could not be confirmed by co-immunoprecipitation assay, we observed the subcellular localization of 10 GFP-tagged selected protein fragments in COS7 cells (Figure 3). As a control, a GFP-tagged selected Fos protein fragment and GFP-HL4-FLAG protein alone (mock) were also transfected. All of the protein fragments that were co-immunoprecipitated with Jun, SNAP19, 4732436F15Rik, 913022H14Rik, Cspg6 and B130050I23Rik, except for 1200008A14Rik, were located mostly in the nucleus, like Fos. On the other hand, the proteins that did not co-immunoprecipitate Jun, Kif5C (region C), Kif5A (region C), Mapre3 and Mapk8ip3, were located mostly in cytoplasm. Mock protein was located ubiquitously in the cells. These results imply that differences in the subcellular localization of the transfected protein fragments could explain the result of the co-immunoprecipitation assay.

Prediction of cellular function

In order to elucidate the cellular roles of the selected proteins, functional annotations of these proteins in public databases were searched from the entries in GO and Refseq. As shown in Figure 4, the 13 unreported proteins and 4 known positives were clustered into five functional groups, microtubule association (Kif5A, Kif5B, Kif5C and Mapre3), kinesin complex (GFAP, Nef3, Kif5A, Kif5B, Kif5C, Mapk8ip3 and Cspg6), chromosome segregation (Cspg6, 9130229H14Rik and 1200008A14Rik), DNA repair (Mapk8ip3, Cspg6 and 9130229H14Rik), and transcriptional regulation (SNAP19, Fos, Jdp2, Atf4 and Jun). Two hypothetical proteins, B130050I23Rik and 4732436F15Rik, have no clear functional annotations (black-bordered boxes in Figure 4).

DISCUSSION

Jun protein is a eukaryotic transcription factor, which plays an important role in a variety of cellular functions, including

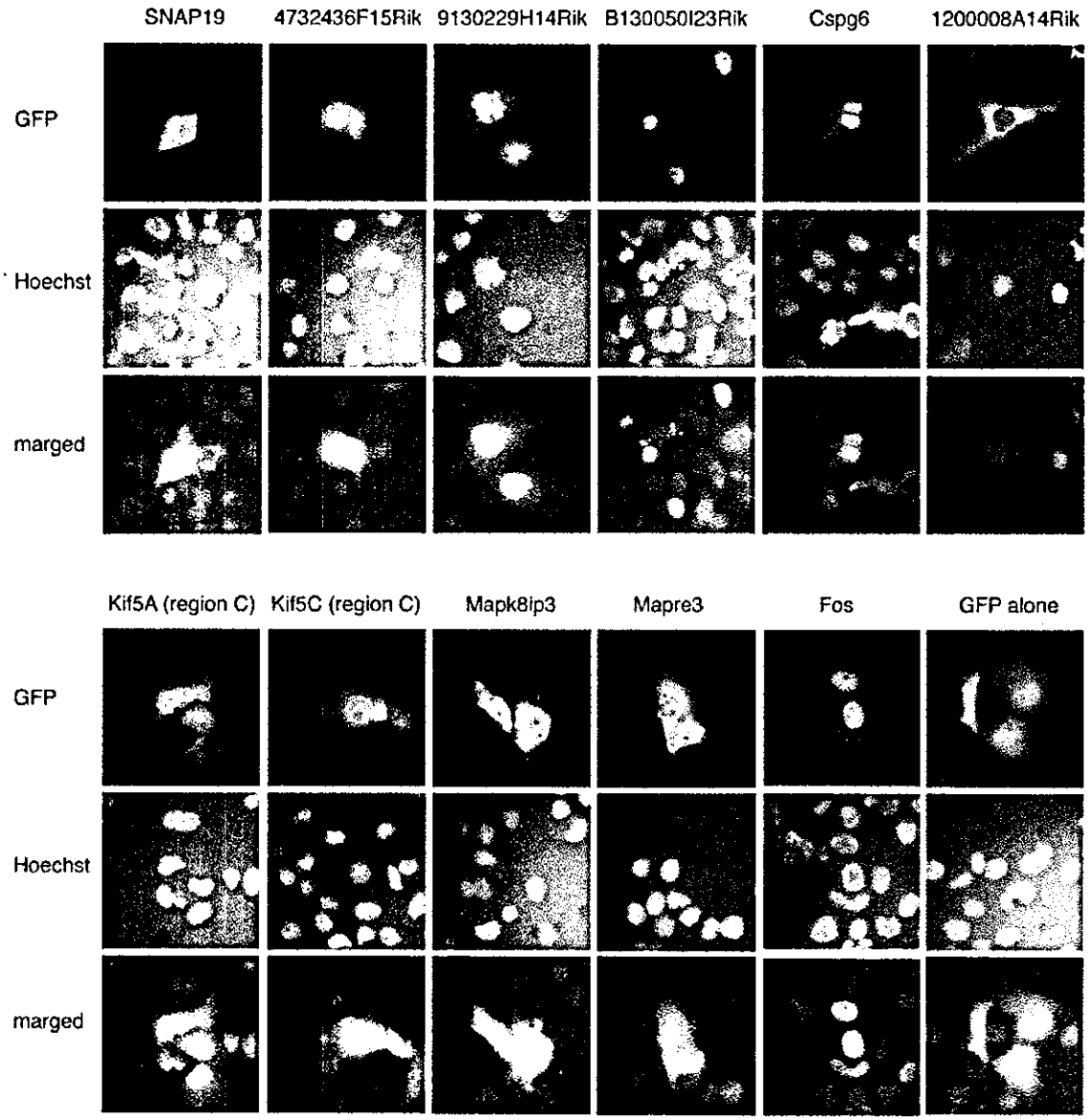

Figure 3. Subcellular localization of the 10 selected protein fragments. COS7 cells were transfected with GFP-tagged selected protein fragments that interacted with Jun *in vitro*. GFP-tagged selected Fos fragment, and GFP-HL4-FLAG alone (negative control). The Fos fragment was used as a positive control of co-localization with Jun, because it was efficiently co-immunoprecipitated with Jun. Upper panels show GFP-tagged proteins. Middle panels show the nucleus stained with Hoechst33342. Lower panels show merged images. GFP and Hoechst33342 appear as green and blue, respectively.

proliferation, differentiation and tumorigenesis (30). The cellular functions of Jun vary according to the interacting partners (24). So far, over 50 Jun-associated proteins have been found in various tissues by using biochemical methods, Y2H assay, and other techniques (24). Jun forms a homodimer and heterodimers with Fos/Jun family proteins such as Fos, Fra1, Fra2, FosB, Jun, JunB and JunD (31–34), and with other bZIP family proteins (24). Jun also interacts directly with many proteins, such as transcriptional co-activators, structurally unrelated DNA binding proteins and nuclear structural components (24). Most of the known Jun-associated proteins are transcriptional regulators.

In this study, we were able to select 20 candidate Jun-associated proteins from a mouse brain cDNA library by using the IVV selection system. Of the 20 candidates, 16 are previously unreported interactions. Of the 16 selected proteins, 10 proteins were confirmed to interact directly with Jun bait protein *in vitro* (Table 1). All 10 proteins, except for Mapre3, contain leucine heptad repeats. This result seems reasonable, because almost all Jun-associated proteins that interact with the bZIP domain of Jun have a leucine zipper motif, which is essential to form heterodimers with Jun (24). Furthermore, 6 of the 10 candidates, SNAP19, Cspg6, 9130229H14Rik, 1200008A14Rik, B130050I23Rik and

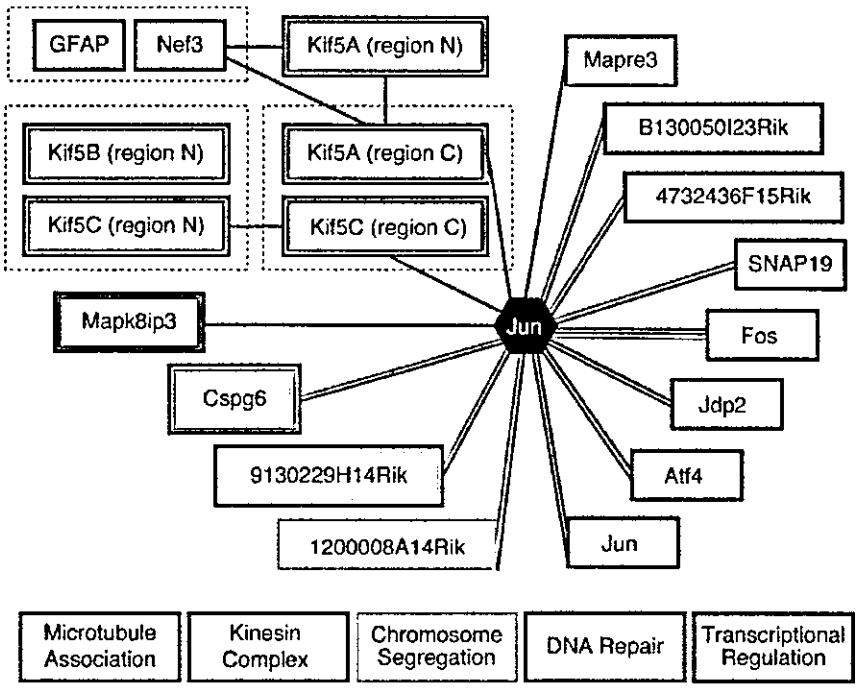

Figure 4. Protein–protein interaction mapping of the selected proteins with functional annotations. Protein–protein interactions confirmed by co-immunoprecipitation and pull-down assay are represented as magenta and blue lines, respectively. Black lines indicate previously reported interactions. Color-bordered boxes represent the functional annotations of the proteins as indicated in the lower panels. Two hypothetical proteins (black-bordered boxes) have no clear functional annotations. Broken-lined squares represent highly homologous protein fragment pairs.

4732436F15Rik, were confirmed to interact with Jun in a cultured cell line by using co-immunoprecipitation assay (Figure 2). We predicted the cellular functions of these proteins by means of functional clustering using annotations.

SNAP19, the most abundant protein (Table 1; 57% of the positives) in this selection, was clustered into the functional group of transcriptional regulation (Figure 4). SNAP19 is known as a 19 kDa subunit of a small nuclear RNA-activating protein complex (35). Previous reports indicate that SNAP19 works in the nucleus as a subunit of the transcriptional regulator protein complex (35). Although no functional or physical relationship between SNAP19 and Jun has been reported previously, our present findings strongly suggest an interaction between SNAP19 and Jun in living cells.

Cspg6, 9130229H14Rik and 1200008A14Rik were clustered into two functional groups, DNA repair and chromosome segregation. This suggests that Jun plays unreported roles in these functions (Figure 4). There are some examples of transcription factors with other non-transcriptional cellular functions; for example, a bZIP transcription factor controls the cell cycle by interacting directly with Cdk2 protein without the involvement of any transcriptional event (36), and an unexpected interaction of Jun with cytoskeletal materials has been reported recently (37). Otherwise our selected proteins may work cooperatively with Jun as transcriptional regulators. For example, Mmip1 protein, an isoform of Cspg6, was reported as a transcriptional suppressor interacting with Mad proteins, a bHLH-ZIP transcriptional regulator family (38,39), implying that Cspg6 protein may also suppress the transcriptional activity of Jun.

Although B130050I23Rik and 4732436F15Rik have no clear annotation, their nuclear localization predicted by the PSORTII program (http://psort.nibb.ac.jp) implies interaction with Jun in the nucleus *in vivo*, and possible functions related to transcriptional regulation. Further *in vivo* experiments are necessary to clarify these proteins' cellular functions.

We could not confirm the interactions between Jun and the other four candidates, Kif5A (region C), Kif5C (region C), Mapk8ip3 and Mapre3, by means of co-immunoprecipitation assay (Figure 2), in spite of the *in vitro* interactions. A possible reason for this would be a difference of subcellular localization between these proteins and Jun. Indeed, all of the proteins that were confirmed to interact with Jun in cultured cells, except for 1200008A14Rik, were located mostly in the nucleus, like Fos protein, a well-known Jun-interactor, while the above-mentioned four proteins were located mostly in cytoplasm (Figure 3), and are known to interact with the cytoskeleton in living cells (40–42). Although the *in vitro* interactions of these four proteins may be biological false positives, biologically significant interaction with Jun cannot be ruled out, because subcellular localizations of some proteins are known to be tightly restricted to a specific phase *in vivo*. For example, Kif17, a closely related paralogous protein of Kif5 family proteins, is located in the nucleus and interacts with ACT protein, a transcriptional co-activator, only at the specific stage of spermatogenesis *in vivo*, and the interaction was only confirmed by immunostaining analysis of mouse testis tissue (43).

So far, genome-wide analyses of protein–protein interactions have been performed by only Y2H and biochemical

methods using MS. The IVV selection system exemplified in this study has several advantages over previous techniques, for example, convenient removability of false positives arising from the selection system itself, availability of a wider range of interacting conditions and availability for analysis of the interactions of toxic proteins. Every current technique for screening of protein–protein interactions has some disadvantages as well as advantages, and therefore the use of a range of different techniques is important to obtain as complete a map as possible of protein–protein interactions in various organisms.

SUPPLEMENTARY MATERIAL

Supplementary Material is available at NAR Online.

ACKNOWLEDGEMENTS

We thank Dr Takashi Takeuchi for experimental advice. This work was supported in part by a Grant-in-Aid for the 21st Century Center of Excellence (COE) Program entitled 'Understanding and Control of Life's Function via Systems Biology (Keio University)' and a Special Coordination Fund of the Ministry of Education, Culture, Sports, Science and Technology, Japan.

REFERENCES

1. Puig,O., Caspary,F., Rigaut,G., Rutz,B., Bouveret,E., Bragado-Nilsson,E., Wilm,M. and Seraphin,B. (2001) The tandem affinity purification (TAP) method: a general procedure of protein complex purification. *Methods*, **24**, 218–229.
2. Fields,S. and Song,O. (1989) A novel genetic system to detect protein–protein interactions. *Nature*, **340**, 245–246.
3. Vidalain,P.O., Boxem,M., Ge,H., Li,S. and Vidal,M. (2004) Increasing specificity in high-throughput yeast two-hybrid experiments. *Methods*, **32**, 363–370.
4. Smith,G.P. (1985) Filamentous fusion phage: novel expression vectors that display cloned antigens on the virion surface. *Science*, **228**, 1315–1317.
5. Bradbury,A.R. and Marks,J.D. (2004) Antibodies from phage antibody libraries. *J. Immunol. Methods*, **290**, 29–49.
6. Hanes,J. and Pluckthun,A. (1997) *In vitro* selection and evolution of functional proteins by using ribosome display. *Proc. Natl Acad. Sci. USA*, **94**, 4937–4942.
7. Mattheakis,L.C., Bhatt,R.R. and Dower,W.J. (1994) An *in vitro* polysome display system for identifying ligands from very large peptide libraries. *Proc. Natl Acad. Sci. USA*, **91**, 9022–9026.
8. Nemoto,N., Miyamoto-Sato,E., Husimi,Y. and Yanagawa,H. (1997) *In vitro* virus: bonding of mRNA bearing puromycin at the 3′-terminal end to the C-terminal end of its encoded protein on the ribosome *in vitro*. *FEBS Lett.*, **414**, 405–408.
9. Miyamoto-Sato,E., Nemoto,N., Kobayashi,K. and Yanagawa,H. (2000) Specific bonding of puromycin to full-length protein at the C-terminus. *Nucleic Acids Res.*, **28**, 1176–1182.
10. Roberts,R.W. and Szostak,J.W. (1997) RNA–peptide fusions for the *in vitro* selection of peptides and proteins. *Proc. Natl Acad. Sci. USA*, **94**, 12297–12302.
11. Yonezawa,M., Doi,N., Kawahashi,Y., Higashinakagawa,T. and Yanagawa,H. (2003) DNA display for *in vitro* selection of diverse peptide libraries. *Nucleic Acids Res.*, **31**, e118.
12. Takahashi,T.T., Austin,R.J. and Roberts,R.W. (2003) mRNA display: ligand discovery, interaction analysis and beyond. *Trends Biochem. Sci.*, **28**, 159–165.
13. Lipovsek,D. and Pluckthun,A. (2004) *In-vitro* protein evolution by ribosome display and mRNA display. *J. Immunol. Methods*, **290**, 51–67.
14. Hammond,P.W., Alpin,J., Rise,C.E., Wright,M. and Kreider,B.L. (2001) *In vitro* selection and characterization of Bcl-X(L)-binding proteins from a mix of tissue-specific mRNA display libraries. *J. Biol. Chem.*, **276**, 20898–20906.
15. Cujec,T.P., Medeiros,P.F., Hammond,P., Rise,C. and Kreider,B.L. (2002) Selection of v-abl tyrosine kinase substrate sequences from randomized peptide and cellular proteomic libraries using mRNA display. *Chem. Biol.*, **9**, 253–264.
16. Miyamoto-Sato,E., Takashima,H., Fuse,S., Sue,K., Ishizaka,M., Tateyama,S., Horisawa,K., Sawasaki,T., Endo,Y. and Yanagawa,H. (2003) Highly stable and efficient mRNA templates for mRNA–protein fusions and C-terminally labeled proteins. *Nucleic Acids Res.*, **31**, e78.
17. Sawasaki,T., Ogasawara,T., Morishita,R. and Endo,Y. (2002) A cell-free protein synthesis system for high-throughput proteomics. *Proc. Natl Acad. Sci. USA*, **99**, 14652–14657.
18. Altschul,S.F., Gish,W., Miller,W., Myers,E.W. and Lipman,D.J. (1990) Basic local alignment search tool. *J. Mol. Biol.*, **215**, 403–410.
19. Thompson,J.D., Higgins,D.G. and Gibson,T.J. (1994) CLUSTAL W: improving the sensitivity of progressive multiple sequence alignment through sequence weighting, position-specific gap penalties and weight matrix choice. *Nucleic Acids Res.*, **22**, 4673–4680.
20. Arai,R., Ueda,H., Kitayama,A., Kamiya,N. and Nagamune,T. (2001) Design of the linkers which effectively separate domains of a bifunctional fusion protein. *Protein Eng.*, **14**, 529–532.
21. Kanagawa,T. (2003) Bias and artifacts in multitemplate polymerase chain reactions (PCR). *J. Biosci. Bioeng.*, **96**, 317–323.
22. Hertveldt,K., Dechassa,M.L., Robben,J. and Volckaert,G. (2003) Identification of Gal80p-interacting proteins by *Saccharomyces cerevisiae* whole genome phage display. *Gene*, **307**, 141–149.
23. Okazaki,Y., Furuno,M., Kasukawa,T., Adachi,J., Bono,H., Kondo,S., Nikaido,I., Osato,N., Saito,R., Suzuki,H. *et al.* (2002) Analysis of the mouse transcriptome based on functional annotation of 60,770 full-length cDNAs. *Nature*, **420**, 563–573.
24. Chinenov,Y. and Kerppola,T.K. (2001) Close encounters of many kinds: Fos–Jun interactions that mediate transcription regulatory specificity. *Oncogene*, **20**, 2438–2452.
25. Doi,N., Takashima,H., Kinjo,M., Sakata,K., Kawahashi,Y., Oishi,Y., Oyama,R., Miyamoto-Sato,E., Sawasaki,T., Endo,Y. *et al.* (2002) Novel fluorescence labeling and high-throughput assay technologies for *in vitro* analysis of protein interactions. *Genome Res.*, **12**, 487–492.
26. Stock,M.F., Guerrero,J., Cobb,B., Eggers,C.T., Huang,T.G., Li,X. and Hackney,D.D. (1999) Formation of the compact confomer of kinesin requires a COOH-terminal heavy chain domain and inhibits microtubule-stimulated ATPase activity. *J. Biol. Chem.*, **274**, 14617–14623.
27. Friedman,D.S. and Vale,R.D. (1999) Single-molecule analysis of kinesin motility reveals regulation by the cargo-binding tail domain. *Nature Cell Biol.*, **1**, 293–297.
28. Seiler,S., Kirchner,J., Horn,C., Kallipolitou,A., Woehlke,G. and Schliwa,M. (2000) Cargo binding and regulatory sites in the tail of fungal conventional kinesin. *Nature Cell Biol.*, **2**, 333–338.
29. Xia,C.H., Roberts,E.A., Her,L.S., Liu,X., Williams,D.S., Cleveland,D.W. and Goldstein,L.S. (2003) Abnormal neurofilament transport caused by targeted disruption of neuronal kinesin heavy chain KIF5A. *J. Cell Biol.*, **161**, 55–66.
30. Shaulian,E. and Karin,M. (2002) AP-1 as a regulator of cell life and death. *Nature Cell Biol.*, **4**, E131–136.
31. Kovary,K. and Bravo,R. (1991) Expression of different Jun and Fos proteins during the G_0-to-G_1 transition in mouse fibroblasts: *in vitro* and *in vivo* associations. *Mol. Cell. Biol.*, **11**, 2451–2459.
32. Lallemand,D., Spyrou,G., Yaniv,M. and Pfarr,C.M. (1997) Variations in Jun and Fos protein expression and AP-1 activity in cycling, resting and stimulated fibroblasts. *Oncogene*, **14**, 819–830.
33. McCabe,L.R., Kockx,M., Lian,J., Stein,J. and Stein,G. (1995) Selective expression of fos- and jun-related genes during osteoblast proliferation and differentiation. *Exp. Cell Res.*, **218**, 255–262.
34. Sonnenberg,J.L., Macgregor-Leon,P.F., Curran,T. and Morgan,J.I. (1989) Dynamic alterations occur in the levels and composition of transcription factor AP-1 complexes after seizure. *Neuron*, **3**, 359–365.
35. Henry,R.W., Mittal,V., Ma,B., Kobayashi,R. and Hernandez,N. (1998) SNAP19 mediates the assembly of a functional core promoter complex (SNAPc) shared by RNA polymerases II and III. *Genes Dev.*, **12**, 2664–2672.
36. Izumiya,Y., Lin,S.F., Ellison,T.J., Levy,A.M., Mayeur,G.L., Izumiya,C. and Kung,H.J. (2003) Cell cycle regulation by Kaposi's

sarcoma-associated herpesvirus K-bZIP: direct interaction with cyclin-CDK2 and induction of G1 growth arrest. *J. Virol.*, **77**, 9652–9661.
37. Luettich,K. and Schmidt,C. (2003) TGFbeta1 activates c-Jun and Erk1 via alphaVbeta6 integrin. *Mol. Cancer*, **2**, 33.
38. Gupta,K., Anand,G., Yin,X., Grove,L. and Prochownik,E.V. (1998) Mmip1: a novel leucine zipper protein that reverses the suppressive effects of Mad family members on c-myc. *Oncogene*, **16**, 1149–1159.
39. Jones,S. and Sgouros,J. (2001) The cohesin complex: sequence homologies, interaction networks and shared motifs. *Genome Biol.*, **2**, RESEARCH0009.
40. Kanai,Y., Okada,Y., Tanaka,Y., Harada,A., Terada,S. and Hirokawa,N. (2000) KIF5C, a novel neuronal kinesin enriched in motor neurons. *J. Neurosci.*, **20**, 6374–6384.
41. Verhey,K.J., Meyer,D., Deehan,R., Blenis,J., Schnapp,B.J., Rapoport,T.A. and Margolis,B. (2001) Cargo of kinesin identified as JIP scaffolding proteins and associated signaling molecules. *J. Cell Biol.*, **152**, 959–970.
42. Nakagawa,H., Koyama,K., Murata,Y., Morito,M., Akiyama,T. and Nakamura,Y. (2000) EB3, a novel member of the EB1 family preferentially expressed in the central nervous system, binds to a CNS-specific APC homologue. *Oncogene*, **19**, 210–216.
43. Macho,B., Brancorsini,S., Fimia,G.M., Setou,M., Hirokawa,N. and Sassone-Corsi,P. (2002) CREM-dependent transcription in male germ cells controlled by a kinesin. *Science*, **298**, 2388–2390.

Rapid Communication

J. Biochem. 137, 121–124 (2005)
DOI: 10.1093/jb/mvi023

Application of Quantitative Real-Time PCR for Monitoring the Process of Enrichment of Clones on *In Vitro* Protein Selection

Kenichi Horisawa, Nobuhide Doi, Hideaki Takashima and Hiroshi Yanagawa*

Department of Biosciences and Informatics, Faculty of Science and Technology, Keio University, 3-14-1 Hiyoshi, Kohoku-ku, Yokohama 223-8522

Received November 29, 2004; accepted December 24, 2004

***In vitro* selection of proteins from cDNA libraries using display technologies, such as the *in vitro* virus method, is a powerful means for the discovery of novel protein interactions. After iterative screening, selected proteins are usually identified and evaluated by cloning and sequencing analysis. Previously we applied real-time PCR for evaluation of the sequences obtained on *in vitro* virus screening. Here, we have presented additional data regarding monitoring of the process of enrichment of selected clones in each round of selection and elimination of false positives by real-time PCR, and have also discussed the utility of the novel method. This approach should also be applicable to other display technologies.**

Key Words: display technology, false positive, *in vitro* virus, mRNA display, real-time PCR.

Abbreviations: IVV, *in vitro* virus; Nrbf2, nuclear receptor binding factor 2; Aes, amino-terminal enhancer of split; Gas5, growth arrest–specific 5.

Display technologies (*1–3*) that link genotype (DNA or RNA) and phenotype (protein) molecules are powerful tools for the discovery of interaction partner proteins for various targets (*e.g.*, proteins, nucleic acids, small-molecular compounds, and drug candidates), using cDNA libraries or artificial random-sequence libraries. Phage display (*4–8*) is the most widely used display technology, and has uncovered many novel functional proteins, protein–protein interactions, and DNA–protein interactions. Furthermore, totally *in vitro* display technologies involving cell-free translation systems, such as ribosome display (*9–11*), mRNA display (*12, 13*), and DNA display (*14–16*), have also been applied for the discovery of novel functional proteins, screening of drug targets (*17*), and protein–protein interaction analysis (*18*).

Figure 1 is a schematic representation of a typical screening procedure involving totally *in vitro* display technologies. Initial libraries of genotype-phenotype linking molecules are affinity-screened and amplified iteratively. The resulting DNA library is cloned into some kind of cloning vector and then sequences are determined by commonly used methods. However, we cannot easily determine much about the abundance ratio or the process of enrichment of the selected clones in each round from only the cloned numbers of the sequences, although such information would be quite useful for evaluating the clones and for optimizing the selection conditions. In addition, the resulting clones often include false positives that are merely abundant in the initial library or that are accidentally picked up in spite of having no binding activity. Therefore, we planned to apply a quantitative real-time PCR technique to monitoring of the process of enrichment of clones on *in vitro* protein selection and elimination of false positives easily by accurately determining the numbers of molecules of each selected DNA in the resulting libraries to confirm the specific enrichment of the sequences.

We recently performed affinity screening of Jun-associated proteins from a mouse brain cDNA library (*19*) using our *in vitro* virus (IVV) method (*12, 13*), one of the mRNA display technologies. In this study, we further analyzed 451 clones including 217 previously analyzed clones which had been picked up from the library on five rounds of iterative screening (*19*). Of the 451 clones, 271 (about 60% of the total analyzed clones) were confirmed to represent intact RNA-protein conjugated molecules without any frame-shift or stop codon on sequence analysis. These 271 clones were clustered into 22 independent sequence groups that were considered to be credible candidates for Jun-associated proteins (Table 1); they included three unreported candidates, nuclear receptor binding factor 2 (Nrbf2) (*20*), amino-terminal enhancer of split (Aes) (*21*), and growth arrest–specific 5 (Gas5) (*22*), together with 19 that we had previously reported (*19*).

We performed real-time PCR analysis to determine the numbers of DNA molecules of the 22 selected sequences (Table 1) in the initial cDNA library, and the libraries obtained on each round of IVV screening in the presence [bait (+)] and absence [bait (–)] of the Jun bait protein (Fig. 2). We found that all of the selected sequences except for those of Aes and Gas5 were enriched in each round of bait (+) selection (Fig. 2A), whereas β-actin (negative control) in the bait (+) selection (Fig. 2A), and all sequences in the bait (–) selection (Fig. 2B) were found not to be enriched. These results indicate that 20 of the 22 sequences had been selected specifically on the basis of affinity for the Jun bait protein, whereas Aes and Gas5 are false positives. Thus, of the three new candidates discovered here, only Nrbf2 was concluded to be a true positive. The interaction between Jun and Nrbf2 was

*To whom correspondence should be addressed. Tel: +81 45 566 1775, Fax: +81 45 566 1440, E-mail: hyana@bio.keio.ac.jp

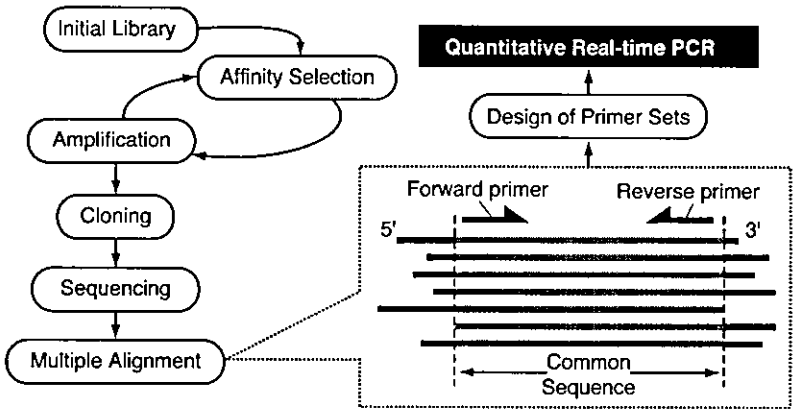

Fig. 1. **A schematic representation of screening with totally *in vitro* display technologies and quantitative real-time PCR analysis.** Initial DNA libraries were constructed by reverse-transcription from poly A (+) RNAs (cDNA library) or chemical synthesis (random-sequence library). Affinity screening and amplification of each library were performed iteratively. After the screening, the resulting library was cloned into a cloning vector and the DNA sequences were determined. The selected DNA sequences were analyzed as described previously (*19*) and were clustered by multiple alignment using the CLUSTALW program (*24*). Primer sets for real-time PCR were designed for each of the clustered sequences. In the case of the sequences of siblings, specific primers were designed based on the common region of the clone encoding each selected sequence. Real-time PCR was performed with a Lightcycler FastStart DNA master SYBR green I kit (Roche) and protein-specific primer sets (the amplicon size was 56 to 200 bp) with a LightCycler (Roche). The standard template DNA was PCR-amplified from each selected sequence on a pDrive vector (Qiagen) using primers 5'M13F (5'-GTTTTCCCAGTCACGACGTTG-3') and 3'M13R (5'-GAAACAGCTATGACCATGATTACG -3'). The numbers of DNA molecules of the selected sequences in 5 ng aliquots (~10^{10} molecules) of DNA libraries were determined.

confirmed by *in vitro* pull-down assays (data not shown), as had been done with other previously confirmed sequences (*19*). Interestingly, the process of enrichment of each selected clone varied. The highest and lowest enrichment ratios in this selection were about 2.0×10^4 and 80-fold, respectively. Furthermore, the process of enrichment of the clones based on the results of real-time PCR is informative for refining the selection protocol, in particular, the selection conditions.

Figure 3 shows the correlation between the abundance ratio of the 22 selected sequences analyzed by real-time PCR, and that found on cloning and sequencing analysis of the library after the fifth round of screening. The two abundance ratios were well correlated in most cases, but not for the Gas5 and Aes sequences (arrows in Fig. 3). Considering that the two sequences were each discovered as a single clone (Table 1), they are certainly false positives.

Real-time PCR is a PCR application that allows accurate quantification of DNA molecules. This technique is based on the PCR kinetics (*23*); the quantification of amplified DNA molecules is performed during the amplification by using intercalators such as a SYBR Green reagent, and the absolute number of DNA molecules is calculated from the results obtained with standards that are observed at the same time. The real-time PCR technique has been used for gene expression analysis and the detection of mutations. In our previous study, we introduced real-time PCR analysis to evaluate the results of *in vitro* selection. In this paper, we have presented additional data regarding monitoring of the process of enrichment of the selected sequences and elimination of false positives by means of real-time PCR. The use of real-time PCR for this purpose has several advantages over previous methods. For example, binding assays, such as *in vitro* pull-down assays and coimmunoprecipitation, are relatively

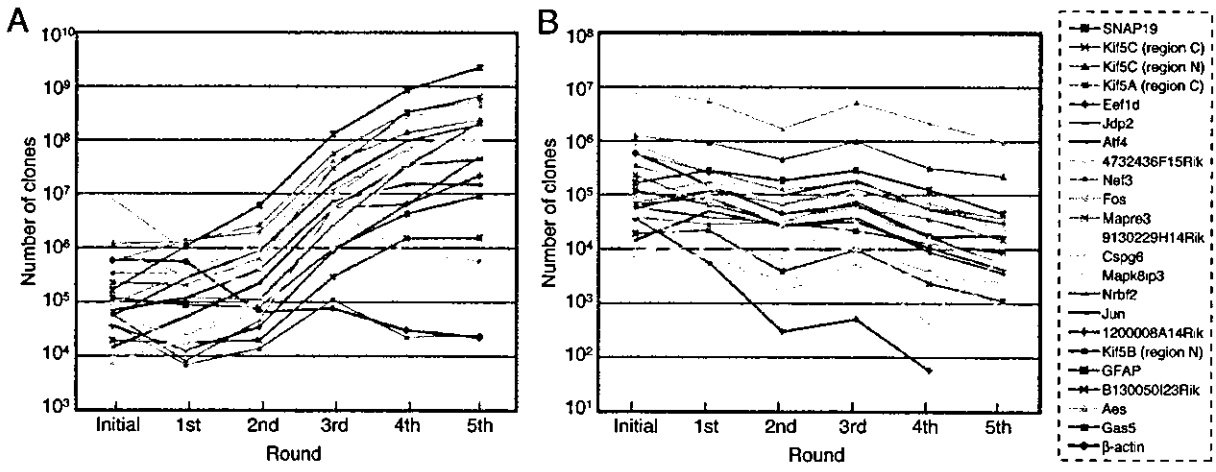

Fig. 2. **Quantitative real-time PCR analysis of the selected sequences in the library obtained on each round.** The numbers of DNA molecules of the 22 specifically selected clones in 5 ng aliquots (~10^{10} molecules) of the libraries, (A) bait (+) and (B) bait (–), obtained on each round were plotted logarithmically. β-Actin was chosen as a negative control.

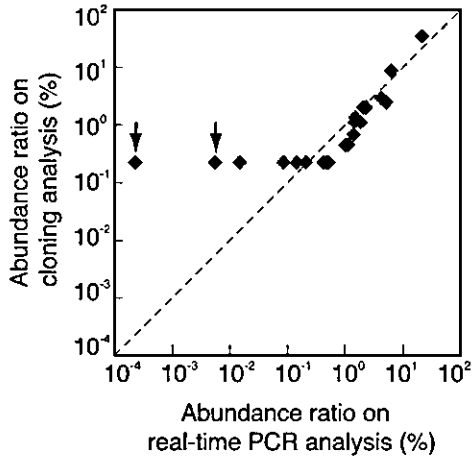

Fig. 3. **Correlation of the abundance ratio on cloning analysis and that on quantitative real-time PCR analysis.** On a logarithmic scale, the vertical axis indicates the abundance ratio on cloning analysis [(number of obtained clones/total number of analyzed clones) × 100 (%)], and the horizontal axis indicates the abundance ratio on real-time PCR analysis [(number of DNA molecules in 5 ng of a DNA library/1.0×10^{10} molecules) × 100 (%)]. The broken line indicates complete correspondence of the two abundance ratios. The arrows indicate Gas5 and Aes from left to right, respectively.

Table 1. **Candidates for Jun-associated proteins selected on IVV screening.**

Gene symbol	Number of clones
SNAP19	155
Kif5C (region C)	39
Kif5A (region C)	13
Kif5C (region N)	11
Eef1d	9
Jdp2	9
Nef3	6
4732436F15Rik	6
Fos	5
Mapre3	3
9130229H14Rik	2
Atf4	2
Cspg6	2
Mapk8ip3	1
Nrbf2	1
Jun	1
1200008A14Rik	1
Kif5B (region N)	1
GFAP	1
B130050I23Rik	1
Aes	1
Gas5	1

tedious to perform. In addition, binding assays involving binary interaction analysis cannot detect indirect interactions, while *in vitro* display technologies can, in principle, detect indirect interactors that form complexes with the bait via direct interactors (*19*).

In summary, we applied real-time PCR to evaluate the sequences of 22 candidate Jun-associated proteins, including three novel candidates picked up on IVV screening. The results show that real-time PCR analysis is a useful tool for monitoring the process of enrichment of specifically selected sequences and for eliminating false positives. This approach should be useful not only for IVV screening, but also for other display technologies, such as ribosome display, DNA display, and phage display.

We wish to thank Dr. S. Tateyama, Dr. E. Miyamoto-Sato and Dr. M. Yonezawa for the useful suggestions during the preparation of the manuscript. This work was supported in part by a Grant-in-Aid for the 21st Century Center of Excellence (COE) Program entitled "Understanding and Control of Life's Function *via* Systems Biology (Keio University)," and special coordination funds from the Ministry of Education, Culture, Sports, Science and Technology of Japan, funds from the New Energy and Industrial Technology Development Organization (NEDO) of Japan, and a Grant-in-Aid for Research on Advanced Medical Technology, Health and Labor Sciences Research Grants from the Ministry of Health, Labor and Welfare of Japan.

REFERENCES

1. Doi, N. and Yanagawa, H. (2001) Genotype-phenotype linkage for directed evolution and screening of combinatorial protein libraries. *Comb. Chem. High Throughput Screen* **4**, 497–509
2. Lipovsek, D. and Plückthun, A. (2004) *In-vitro* protein evolution by ribosome display and mRNA display. *J. Immunol. Methods* **290**, 51–67
3. Kondo, A. and Ueda, M. (2004) Yeast cell-surface display–applications of molecular display. *Appl. Microbiol. Biotechnol.* **64**, 28–40
4. Smith, G.P. (1985) Filamentous fusion phage: novel expression vectors that display cloned antigens on the virion surface. *Science* **228**, 1315–1317
5. Fujii, I., Fukuyama, S., Iwabuchi, Y., and Tanimura, R. (1998) Evolving catalytic antibodies in a phage-displayed combinatorial library. *Nat. Biotechnol.* **16**, 463–467
6. Faix, P.H., Burg, M.A., Gonzales, M., Ravey, E.P., Baird, A., and Larocca, D. (2004) Phage display of cDNA libraries: enrichment of cDNA expression using open reading frame selection. *Biotechniques* **36**, 1018–1022, 1024, 1026–1029
7. Hagiwara, H., Kunihiro, S., Nakajima, K., Sano, M., Masaki, H., Yamamoto, M., Pak, J.W., Zhang, Y., Takase, K., Kuwabara, I. *et al.* (2002) Affinity selection of DNA-binding proteins from yeast genomic DNA libraries by improved lambda phage display vector. *J. Biochem.* **132**, 975–982
8. Yamauchi, A., Nakashima, T., Tokuriki, N., Hosokawa, M., Nogami, H., Arioka, S., Urabe, I., and Yomo, T. (2002) Evolvability of random polypeptides through functional selection within a small library. *Protein Eng.* **15**, 619–626
9. Mattheakis, L.C., Bhatt, R.R., and Dower, W.J. (1994) An in vitro polysome display system for identifying ligands from very large peptide libraries. *Proc. Natl Acad. Sci. USA* **91**, 9022–9026
10. Hanes, J. and Pluckthun, A. (1997) *In vitro* selection and evolution of functional proteins by using ribosome display. *Proc. Natl Acad. Sci. USA* **94**, 4937–4942
11. Zhou, J.M., Fujita, S., Warashina, M., Baba, T. and Taira, K. (2002) A novel strategy by the action of ricin that connects phenotype and genotype without loss of the diversity of libraries. *J. Amer. Chem. Soc.* **124**, 538–543
12. Nemoto, N., Miyamoto-Sato, E., Husimi, Y., and Yanagawa, H. (1997) *In vitro* virus: bonding of mRNA bearing puromycin at the 3'-terminal end to the C-terminal end of its encoded protein on the ribosome in vitro. *FEBS Lett.* **414**, 405–408

13. Miyamoto-Sato, E., Takashima, H., Fuse, S., Sue, K., Ishizaka, M., Tateyama, S., Horisawa, K., Sawasaki, T., Endo, Y., and Yanagawa, H. (2003) Highly stable and efficient mRNA templates for mRNA-protein fusions and C-terminally labeled proteins. *Nucleic Acids Res.* **31**, e78
14. Doi, N. and Yanagawa, H. (1999) STABLE: protein-DNA fusion system for screening of combinatorial protein libraries *in vitro*. *FEBS Lett.* **457**, 227–230
15. Yonezawa, M., Doi, N., Kawahashi, Y., Higashinakagawa, T., and Yanagawa, H. (2003) DNA display for *in vitro* selection of diverse peptide libraries. *Nucleic Acids Res.* **31**, e118
16. Odegrip, R., Coomber, D., Eldridge, B., Hederer, R., Kuhlman, P.A., Ullman, C., FitzGerald, K., and McGregor, D. (2004) CIS display: *In vitro* selection of peptides from libraries of protein-DNA complexes. *Proc. Natl Acad. Sci. USA* **101**, 2806–2810
17. McPherson, M., Yang, Y., Hammond, P.W., and Kreider, B.L. (2002) Drug receptor identification from multiple tissues using cellular-derived mRNA display libraries. *Chem. Biol.* **9**, 691–698
18. Hammond, P.W., Alpin, J., Rise, C.E., Wright, M., and Kreider, B.L. (2001) *In vitro* selection and characterization of Bcl-X(L)-binding proteins from a mix of tissue-specific mRNA display libraries. *J. Biol. Chem.* **276**, 20898–20906
19. Horisawa, K., Tateyama, S., Ishizaka, M., Matsumura, N., Takashima, H., Miyamoto-Sato, E., Doi, N., and Yanagawa, H. (2004) *In vitro* selection of Jun-associated proteins using mRNA display. *Nucleic Acids Res.* **32**, e169
20. Yasumo, H., Masuda, N., Furusawa, T., Tsukamoto, T., Sadano, H., and Osumi, T. (2000) Nuclear receptor binding factor-2 (NRBF-2), a possible gene activator protein interacting with nuclear hormone receptors. *Biochim. Biophys. Acta* **1490**, 189–197
21. Miyasaka, H., Choudhury, B.K., Hou, E.W., and Li, S.S. (1993) Molecular cloning and expression of mouse and human cDNA encoding AES and ESG proteins with strong similarity to Drosophila enhancer of split groucho protein. *Eur. J. Biochem.* **216**, 343–352
22. Smith, C.M. and Steitz, J.A. (1998) Classification of gas5 as a multi-small-nucleolar-RNA (snoRNA) host gene and a member of the 5′-terminal oligopyrimidine gene family reveals common features of snoRNA host genes. *Mol. Cell. Biol.* **18**, 6897–6909
23. Higuchi, R., Fockler, C., Dollinger, G., and Watson, R. (1993) Kinetic PCR analysis: real-time monitoring of DNA amplification reactions. *Biotechnology* **11**, 1026–1030
24. Thompson, J.D., Higgins, D.G., and Gibson, T.J. (1994) CLUSTAL W: improving the sensitivity of progressive multiple sequence alignment through sequence weighting, position-specific gap penalties and weight matrix choice. *Nucleic Acids Res.* **22**, 4673–4680